Chemosphere 288 (2022) 132536

Contents lists available at ScienceDirect

Chemosphere

journal homepage: www.elsevier.com/locate/chemosphere

Toxicity of α-Ag_2WO_4 microcrystals to freshwater microalga *Raphidocelis subcapitata* at cellular and population levels

Cínthia Bruno de Abreu [a,b,*], Renan Castelhano Gebara [a,b], Larissa Luiza dos Reis [a,b], Giseli Swerts Rocha [c], Lays de Oliveira Gonçalves Alho [a,b], Laís Mendes Alvarenga [d], Luciano Sindra Virtuoso [d], Marcelo Assis [e], Adrislaine da Silva Mansano [a,b], Elson Longo [e], Maria da Graça Gama Melão [a]

[a] Department of Hydrobiology, Federal University of São Carlos (UFSCar), Rodovia Washington Luís, Km 235, 13565-905, São Carlos, SP, Brazil
[b] Post-Graduate Program in Ecology and Natural Resources (PPGERN), Federal University of São Carlos (UFSCar), Rodovia Washington Luís, Km 235, 13565-905, São Carlos, SP, Brazil
[c] Department of Hydraulic and Sanitation (NEEA/CRHEA/SHS), São Carlos School of Engineering, University of São Paulo, Avenida Trabalhador São-Carlense 400, 13560-970, São Carlos, SP, Brazil
[d] Chemistry Institute - Federal University of Alfenas (UNIFAL-MG), Gabriel Monteiro da Silva, 700, Centro, 37130-000, Alfenas, MG, Brazil
[e] Center for Development of Functional Materials (CDMF), Federal University of São Carlos - (UFSCar), P.O, Box 676, 13565-905, São Carlos, SP, Brazil

HIGHLIGHTS

- α-Ag_2WO_4–R (rod) was more toxic than α-Ag_2WO_4–C (cube) to *R. subcapitata*.
- At 96 h, there was total population growth inhibition at the highest concentrations.
- Both microcrystal shapes altered the cellular complexity of *R. subcapitata*.
- α-Ag_2WO_4 exposure led to decreased chlorophyll *a* fluorescence at all concentrations.
- α-Ag_2WO_4–R induced ROS production at the highest concentration (31.76 μg L^{-1}).

ARTICLE INFO

Handling Editor: Willie Peijnenburg

Keywords:
ROS
Chlorophyceae
α-Ag_2WO_4
Ecotoxicity
Silver microparticles
Growth inhibition

ABSTRACT

Silver-based materials have microbicidal action, photocatalytic activity and electronic properties. The increase in manufacturing and consumption of these compounds, given their wide functionality and application, is a source of contamination to freshwater ecosystems and causes toxicity to aquatic biota. Therefore, for the first time, we evaluated the toxicity of the silver tungstate (α-Ag_2WO_4), in different morphologies (cube and rod), for the microalga *Raphidocelis subcapitata*. To investigate the toxicity, we evaluated the growth rate, cell complexity and size, reactive oxygen species (ROS) production and chlorophyll *a* (Chl a) fluorescence. The α-Ag_2WO_4 – R (rod) was 1.7 times more toxic than α-Ag_2WO_4–C (cube), with IC_{10} and IC_{50} values of, respectively, 8.68 ± 0.91 μg L^{-1} and 13.72 ± 1.48 μg L^{-1} for α-Ag_2WO_4 – R and 18.60 ± 1.61 μg L^{-1} and 23.47 ± 1.16 μg L^{-1} for α-Ag_2WO_4–C. The release of silver ions was quantified and indicated that the silver ions dissolution from the α-Ag_2WO_4 – R ranged from 34 to 71%, while the Ag ions from the α-Ag_2WO_4–C varied from 35 to 97%. The α-Ag_2WO_4–C induced, after 24 h exposure, the increase of ROS at the lowest concentrations (8.81 and 19.32 μg L^{-1}), whereas the α-Ag_2WO_4 – R significantly induced ROS production at 96 h at the highest concentration (31.76 μg L^{-1}). Both microcrystal shapes significantly altered the cellular complexity and decreased the Chl *a* fluorescence at all tested concentrations. We conclude that the different morphologies of α-Ag_2WO_4 negatively affect the microalga and are important sources of silver ions leading to harmful consequences to the aquatic ecosystem.

* Corresponding author. Department of Hydrobiology, Federal University of São Carlos (UFSCar), Rodovia Washington Luís, Km 235, 13565-905, São Carlos, SP, Brazil.
E-mail address: cinthiaabreu123@gmail.com (C.B. Abreu).

https://doi.org/10.1016/j.chemosphere.2021.132536
Received 20 August 2021; Received in revised form 7 October 2021; Accepted 8 October 2021
Available online 9 October 2021

1. Introduction

Recently, silver-based materials have drawn attention due to their excellent antimicrobial properties (Nobre et al., 2019; Penha et al., 2020). The high production of these materials increases the availability in the environment presenting a health risk to aquatic ecosystems leading to damage to different species of organisms, such as bacteria (Fabrega et al., 2009), microcrustaceans (Sørensen et al., 2016), fish (Griffitt et al., 2011), aquatic plants (Varga et al., 2018) and microalgae (Kleiven et al., 2019; Ribeiro et al., 2015; Sendra et al., 2017). Among these materials, the silver tungstate (α-Ag_2WO_4) is a multifunctional material with physical and chemical properties relevant for different functions (Laier et al., 2020). Silver tungstates are widely used in the microbial (Nobre et al., 2019; Macedo et al., 2019; Laier et al., 2020; Alvarez-Roca et al., 2021) and antitumor activity (Lin et al., 2012; Assis et al., 2019), sensors (Silva et al., 2014; Muthamizh et al., 2015, Silva et al., 2016), magnetic materials (Assis et al., 2020) and photocatalysts areas (Arumugam et al., 2020; Ayappan et al., 2020; Cruz et al., 2020; Dai et al., 2010; Macedo et al., 2019).

This composite has been widely studied in fighting antibiotic resistant bacteria and fungi, such as *Staphylococcus aureus* (MRSA) and *Candida albicans* (Foggi et al., 2017a, 2017b). Besides that, this composite has the potential for gas detection and luminescence (Penha et al., 2020), and even to decontaminate organic dyes in polluted waters through photocatalysis (Macedo et al., 2018). Since α-Ag_2WO_4 becomes the focus of many studies, it is essential to know its impact on the environment, especially in aquatic environments.

The activity of α-Ag_2WO_4 is related to its size, morphology, composition and surface structure (Laier et al., 2020; Assis et al., 2021). Among these factors, the morphology of the compound is a major one because it is the surface that determines the number of active sites, which consequently significantly alters its properties (Macedo et al., 2018). Another crucial factor to be considered, regarding its toxicity, is the amount of ions released by the α-Ag_2WO_4. Zhao et al. (2012) emphasizes the importance of evaluating the Ag release as a result of particle surface changes in ecotoxicity studies, because the toxicity is often caused by the interaction of Ag ions with biological molecules, such as proteins and enzymes (Navarro et al., 2008). In relation to the environmental concentration threshold determined by the Environmental Agencies, it corresponds only to the ionic silver level. The ionic silver concentration limit in the United States is 3.2 μg L^{-1}, in Canada 0.1 μg L^{-1}, in Australia and New Zealand 0.05 μg L^{-1}, and in Scotland 0.1 μg L^{-1} (Kwak et al., 2015). The World Health Organization (2011) determined that the ionic silver limit up to 0.1 mg L^{-1} in drinking water poses no health risks (Lalau et al., 2020). In Brazil, the National Council for the Environment - CONAMA 357/05 (BRASIL, 2005) sets a limit of up to 0.01 mg L^{-1} of silver in freshwater.

Microalgae are essential in aquatic ecosystems as they are primary producers, producing oxygen for the maintenance of life of other organisms (Ribeiro et al., 2015; Wang et al., 2016) . As they are at the base of aquatic food webs, damage to these organisms can impact higher trophic levels and the entire ecosystem (Munawar et al., 1989). Especially for microalgae, it is widely known and discussed in the literature that silver-based materials can cause toxicity and adverse effects, such as oxidative stress, DNA damage and growth inhibition (He et al., 2012; Huang et al., 2016; Lekamge et al., 2020; Rogers et al., 2018; Sørensen et al., 2016). Furthermore, silver ions are extremely toxic to aquatic organisms, as they interact with biological molecules, compromising their functions (Odzak et al., 2017), in particular photosynthetic organisms.

In this study, we aimed to investigate the toxicity caused by two morphologies of α-Ag_2WO_4, cube (α-Ag_2WO_4–C) and rod (α-Ag_2WO_4 - R) on the microalgae *Raphidocelis subcapitata*. This species is a cosmopolitan Chlorophyceae widely used in ecotoxicological studies due to its sensitivity to several contaminants (Gebara et al., 2020; Mansano et al., 2017; Reis et al., 2021). Moreover, it responds quickly to environmental changes (Almeida et al., 2019). We evaluated the toxicity of the isolated composites from multiple endpoints at the population (growth rate), morphological (cell complexity and size) and intracellular level (Chl *a* fluorescence and ROS production). This is the first study reporting the effects of α-Ag_2WO_4, in different morphologies for an aquatic organism. Understanding the toxicity mechanism of these compounds on a primary producer provides relevant information for the proper and cautious use of silver-based materials. In addition, our results are useful in guiding norms and resolutions with safe thresholds for freshwater ecosystems.

2. Material and methods

2.1. Synthesis and characterization of α-Ag_2WO_4

The samples of α-Ag_2WO_4 were synthesized by the coprecipitation (CP) method in aqueous medium, both to form rod and cube morphologies (Macedo et al., 2018). For α-Ag_2WO_4 - R, two solutions were prepared: (i) 1.10^{-3} mol of $Na_2WO_4{\cdot}2H_2O$ (Sigma-Aldrich, 99.9% purity) in 100 ml of distilled water and (ii) 2.10^{-3} mol of $AgNO_3$ (Cennabras, 99.8% purity) in 100 ml of distilled water. Both were heated to 70 °C and then solution (ii) was added to solution (i) under magnetic stirring. After that, the formation of a white precipitate was observed, which was left under stirring for 10 min. The precipitate was then separated by centrifugation (1 min–4400 rpm), washed five times with distilled water until pH ~ 7, and dried for 12 h at 60 °C. To obtain the α-Ag_2WO_4–C, 1 g of sodium dodecyl sulfate (Sigma-Aldrich, 99% purity) was added to the solution (i) before adding solution (ii). The samples were characterized by X-ray diffraction (XRD) using a D/Max-2500PC diffractometer (Rigaku) with Cu Kα radiation (λ = 1.5406 Å) and the morphologies of the samples were observed by field emission scanning electronic microscopy (FE-SEM) operated at 10 kV (Supra 35-VP, Carl Zeiss). The hydrodynamic size, polydispersity index (PdI) and zeta potential of the particles were measured in exposure medium and in ultrapure water at 0 h and 96 h by dynamic light scattering (DLS) using Zetasizer Nano ZS90, Malvern.

2.2. Silver concentrations and ion release

The silver concentrations in α-Ag_2WO_4 test solutions used in the toxicity tests (Tables S1 and S2, Supplementary material) were determined by inductively coupled plasma mass spectrometry (ICP-MS PerkinElmer NexION, 2000), where the limits of quantification and detection were 0.0084 and 0.0028 μg L^{-1}, respectively. To detect the free silver ions, each sample was centrifuged (Eppendorf 5702 R, Germany) at 4400 rpm for 60 min using a 3 kDa Amicon centrifugal filter (Merck Millipore, Darmstadt, Germany) to remove α-Ag_2WO_4 particles or agglomerates. The filtered volumes were subsequently quantified using ICP-MS and therefore the fraction <3 kDa was considered dissolved Ag.

2.3. Algae culture and toxicity tests

The *R. subcapitata* inoculum was obtained from the Department of Ecology and Evolutionary Biology (DEBE, Federal University of São Carlos - UFSCar, São Carlos - SP, Brazil) and cultivated in culture medium CHU-12 (Chu, 1942) (Table S3, Supplementary material) at 25 ± 1 °C, with light intensity (≅ 130 μmol photon m^{-2} s^{-1} LED light) and 12 h/12 h of light/dark photoperiod. The room temperature was 24.5–25 °C and the pH values were around 7–8.5 and did not vary by more than 1.5 units. The particles were dispersed in ultrapure water using a bath sonicator (Ultra cleaner 1400 Unique) for 30 min and subsequently, were used to prepare test solutions. The algal cultures in the exponential growth phase were inoculated in a concentration of 1 × 10^5 cells ml^{-1} in 500 ml polycarbonate erlenmeyers containing 250 ml of test solutions. *R. subcapitata* was exposed for 96 h to concentrations of 0.00, 8.81, 19.32, 27.78, 32.87 and 36.25 μg L^{-1} for α-Ag_2WO_4–C and

0.00, 4.11, 5.84, 10.55, 10.67 and 31.76 μg L^{-1} for α-Ag_2WO_4-R. These concentrations were chosen based on preliminary tests. The toxicity tests followed the OECD (2006) guidelines, and 3 tests were performed, each one with triplicates for control and treatments.

2.4. Flow cytometric analysis

For algal cell counting, 1.8 ml samples were fixed with formaldehyde buffered with borax (1% final concentration) at room temperature. In the following step, the samples were frozen in liquid nitrogen and stored at −20 °C until analysis. For ROS analysis, 495 μL of each sample and 5 μL of DCFH-DA (2′,7′-Dichlorofluorescein diacetate, Sigma Aldrich) diluted in dimethylsulfoxide (10^4 μM) were aliquoted, with a final concentration of 10 μM. After that, the samples were kept in the dark for 60 min and immediately analyzed by flow cytometry. Cell density and ROS measurements were performed in a FACSCalibur cytometer (Becton Dickinson, San Jose, CA, USA) with a 15 mW argon-ion laser (488 nm excitation), using 6 μm fluorescent beads as an internal standard (Fluoresbrite carboxylate microspheres; Polysciences, Warrington, Pennsylvania, USA). The cells of *R. subcapitata* were identified using the parameter side scatter (SSC–H) *versus* red fluorescence (FL3-H), according to Sarmento et al. (2008), and for relative ROS, the parameters FL3-H and FL1-H (green fluorescence) were used. The relative values of FL3-H (Chl *a* fluorescence), SSC-H (cell complexity), and FSC-H (cell size) of *R. subcapitata* were calculated using the measurements of the fluorescent beads, as described in Mansano et al. (2017). The data were analyzed in FlowJo V10 software. Equations (1) and (2) were used to calculate the relative ROS (Hong et al., 2009). The relative growth rates (RGR) were determined using equation (3) (Bao et al., 2011), where N_t is the cell density at time t; N_0 is the initial cell density and t is the exposure time. Thus, growth inhibition % was calculated by comparing the population growth rates of controls (considered 100%) with the treatments. The percent inhibition in yield (%Iy) was calculated for each treatment replicate according equation (4) (OECD, 2011), where Y_C is mean value for yield in the control group and Y_T is the value for yield for the treatment replicate.

$$FL1\text{-}H_{relative} = \log (FL1\text{-}H \text{ of samples}) / \log (FL1\text{-}H \text{ of beads}) \quad \text{(eq. 1)}$$

$$ROS_{relative}\,(\%) = (FL1\text{-}H_{relative\ [treatments]} / FL1\text{-}H_{relative\ [control\ group]}) \text{ X } 100 \quad \text{(eq. 2)}$$

$$RGR = (N_t\text{–}N_0)_{\ Treatment} / (N_t\text{–}N_0)_{\ Control} \quad \text{(eq. 3)}$$

$$\%I_y = (Y_C - Y_T) / Y_C \text{ X } 100 \quad \text{(eq. 4)}$$

2.5. Data analysis

The inhibitory concentrations (IC_{10} and IC_{50}) based on relative growth rates were calculated by non-linear regression logistic curves using Statistica 7.0 software (Statsoft Inc, 2004). Statistical analyses were performed in the SigmaPlot software version 11.0 (Systat, 2008). To assess the differences between control and treatments, normal distributed data were analyzed with one-way ANOVA, followed by Dunnett's post-hoc multiple comparison test. For non-normal data, Kruskal-Wallis test and multiple comparisons with Dunn's test were performed. Statistical significance level was defined as $p < 0.05$.

3. Results and discussion

3.1. Characterization of particles and ion release

The characterization of α-Ag_2WO_4 particles by XRD is shown in Fig S1 Supplementary Material. For both α-Ag_2WO_4 - R and α-Ag_2WO_4–C samples, the phase of α-Ag_2WO_4 with an orthorhombic structure was obtained, according to the Inorganic Crystal Structure Database (ICSD) file no. 293487 (Cavalcante et al., 2012). This structure belongs to the spatial group *Pn2n*, and is formed by Ag ([AgO_x], x = 2, 4, 6 and 7) and W ([WO_6]) complexes clusters. (Assis et al., 2018, 2019). No additional phases were observed, showing that the material obtained has a high purity.

FE-SEM images of the samples are shown in Fig. 1. For α-Ag_2WO_4–C, the homogeneous formation of microstructured cubes was observed, with an average length of 0.83 ± 0.21 μm and an average width of 0.75 ± 0.17 μm. For α-Ag_2WO_4-R, the homogeneous formation of rods with a hexagonal face were obtained, with an average length of 1.22 ± 0.10 μm and an average width of 0.23 ± 0.70 μm.

The data of microparticle characterization in culture medium and in ultrapure water are summarized in Tables S4 and S5 (Supplementary material). The hydrodynamic diameter of particles dispersed in the culture medium ranged from 589 to 1475 nm for α-Ag_2WO_4–C and from 202 to 735 nm for α-Ag_2WO_4 - R. The results of the zeta potential, at 0 h and 96 h for both microparticles, showed a tendency for rapid aggregation and incipient instability. On average, the values found did not exceed −10 mV. Suspensions considered stable in aqueous solutions have zeta potential values higher +30 mV and below −30 mV (Stensberg et al., 2011). In our study, we found slightly negative values and close to zero which confirms the electrostatic instability (Lodeiro et al., 2017; Kleiven et al., 2018, 2019). The PdI values were higher than 0.510 ± 0.22 for α-Ag_2WO_4–C and higher than 0.421 ± 0.07 for α-Ag_2WO_4-R, which indicated that the microparticles formed aggregates/agglomerates.

We observed that the free silver ion release from the samples varied (Fig. 2). The dissolution of silver ions from increasing concentrations of α-Ag_2WO_4 – R followed a sigmoidal behavior (Fig. 2A), while the Ag ions from the α-Ag_2WO_4–C had an increasing linear trend (Fig. 2B). For α-Ag_2WO_4–C the fraction of dissolved silver ions in the suspension ranged from 34.24% (which corresponds to 5.24 μg Ag L^{-1}, at the concentration of 32.87 μg L^{-1}) to 71.22% (corresponds to 2.95 μg Ag L^{-1}, at the concentration of 8.81 μg L^{-1}) (Table S1, Supplementary material). For α-Ag_2WO_4 – R, the fraction of dissolved silver ions in the suspension ranged from 35.52% (5.25 μg Ag L^{-1} at concentration 31.76 μg L^{-1}) to 96.66% (corresponding to 4.55 μg Ag L^{-1} at concentration 10.67 μg L^{-1}) (Table S2, Supplementary material).

The ion dissolution of the particles is related to the surface area, size, shape, structure and it is dependent on the methodology used in the synthesis, functionalization, and medium in which they were dispersed (Lopes et al., 2014; Lekamge et al., 2020). There are discussions about the importance of particle size, in which very small particles have greater dissolution, due to the surface area, i.e., nano-sized particles compared to micro-sized particles have a greater surface area and greater ion dissolution (Beer et al., 2012; Dobias and Bernier-Latmani, 2013; Sendra et al., 2017). However, our data highlight that even though they are microcrystal, there was a large amount of silver ion released from the treatments and the α-Ag_2WO_4 particles were important sources of free silver ion, causing toxicity to the algal cells, as discussed in the following topics.

Toxicity of α-Ag_2WO_4 microparticles.

3.1.1. Growth inhibition

The α-Ag_2WO_4 - R and α-Ag_2WO_4–C caused negative effects on the relative growth rates of *R. subcapitata* (Fig. 3). After 96 h of exposure to α-Ag_2WO_4–C, the population growth was significantly decreased in concentrations of 27.78 μg L^{-1}, 32.87 μg L^{-1} and 36.25 μg L^{-1} (Dunnett's test, $p < 0.05$) (Fig. 3A). Regarding the α-Ag_2WO_4 – R, the algae growth was significantly reduced at the concentrations of 10.55 μg L^{-1}, 10.67 μg L^{-1} and 31.76 μg L^{-1} when compared to the control (Dunnett's test, $p < 0.05$) (Fig. 3B). We observed a relationship between availability of silver ions released from microcrystal and growth inhibition. Fig. 3C and D shows the silver ion concentrations in each α-Ag_2WO_4–C and α-Ag_2WO_4 – R treatment, respectively.

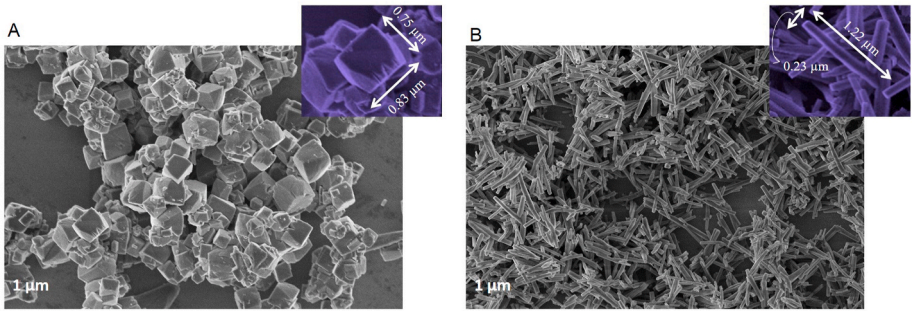

Fig. 1. FE-SEM images of α-Ag_2WO_4–C (A) and α-Ag_2WO_4 – R (B).

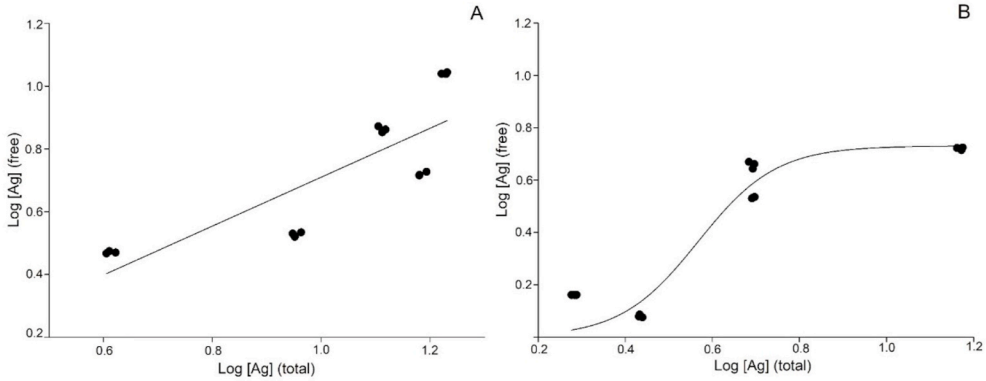

Fig. 2. Total silver concentration *versus* free silver ion concentration in α-Ag_2WO_4–C (A) (Linear regression equation f = −0.0686 + 0.7786*x, with $r^2 = 0.68$) and α-Ag_2WO_4 - R (B) (Sigmoid regression equation f = 0.7307/(1 + exp (-(x-0.5674)/0.0893, with $r^2 = 0.91$).

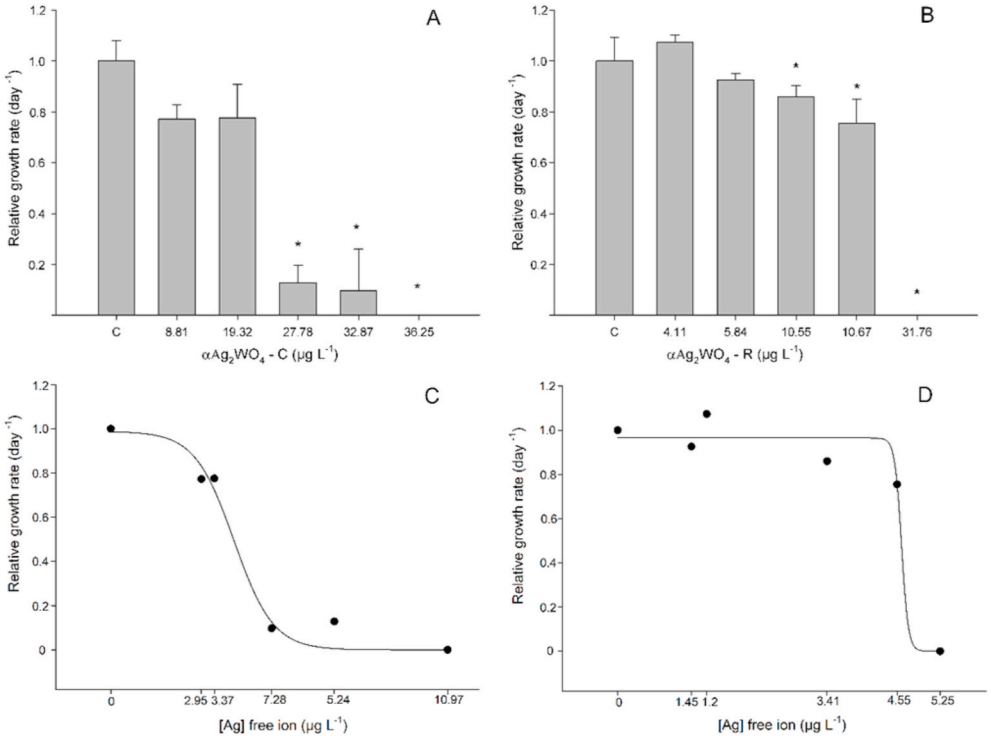

Fig. 3. Relative growth rates (mean ± standard deviation) of *Raphidocelis subcapitata* after 96 h exposure to different concentrations of α-Ag_2WO_4–C (A) and α-Ag_2WO_4 - R (B). Relative growth rates (mean ± standard deviation) of *Raphidocelis subcapitata* versus concentration of free ions (in relation to silver) of α-Ag_2WO_4–C (C) (Sigmoid regression equation f = 0.9883/(1 + exp (-(x-4.0112)/-0.6389), with $r^2 = 0.96$) and α-Ag_2WO_4 – R (D) (Sigmoid regression equation f = 0.9648/(1 + exp (-(x-4.6207)/-0.0552)), with $r^2 = 0.94$). Concentrations are expressed in µg L^{-1}, where: C = control group and asterisks represent a significant difference (Dunnett's test, $p < 0.05$) of treatments compared to the control group.

The percent of yield inhibition (%Iy) are summarized in Table S6 and S7 (Supplementary material). According to the OECD, this parameter is calculated based on biomass and is required by some countries to meet regulatory aspects, therefore considered as an additional variable. In this study, we observed the significant increase (Dunnett's test, $p < 0.05$) of percent inhibition in yield (%Iy) in the α-Ag_2WO_4–C and α-Ag_2WO_4 – R treatments when compared to the control group, like the results found by Sohn et al. (2015).

The IC_{10} and IC_{50} values were, respectively, 18.60 ± 1.61 μg L^{-1} and 23.47 ± 1.16 μg L^{-1} for α-Ag_2WO_4–C, and 8.68 ± 0.91 μg L^{-1} and 13.72 ± 1.48 μg L^{-1} for α-Ag_2WO_4 – R, showing a higher toxicity of the rod of 1.7 times in comparison to the α-Ag_2WO_4–C morphology. The higher toxicity of α-Ag_2WO_4 – R can be explained by the existing differences in the shape and surfaces of each compound. These surfaces are closely related to the number of active sites and consequently to their properties (Laier et al., 2020).

In the theoretical study by Macedo et al. (2018), it is detailed that α-Ag_2WO_4 has differences in the surface energy of the facets that make up each microcrystal morphology. The cubic morphology has a combination of surfaces (010), (100) and (001) and is obtained by using sodium dodecyl sulfate (SDS), which is responsible for stabilizing the surfaces (100) and (001). In addition, the use of SDS prevents the emergence of the predominant surface of the hexagonal rod-like morphology (010), (001) and (101). The different surfaces between the samples are (101) for α-Ag_2WO_4 - R and (100) for α-Ag_2WO_4–C. The surface (101) has 4 vacant clusters on its surface ([$AgO_3.3V_o$], [$AgO_5.2V_o$] and two [WO_5. V_o]) while the surface (100) has 3 vacant clusters on its surface ([$AgO_3.3V_o$], [$AgO_5.2V_o$] and one [WO_5. V_o]). These clusters represent the centers of surface activity of these surfaces, they are considered as their active sites, and influence the ability of materials to interact with the alga and the release of silver ions. The difference in these surfaces of sample explains the greater toxicity of α-Ag_2WO_4 - R in inhibiting the growth of *R. subcapitata* as the greater number of active sites of this compound are closely related to the surface. Thereby, we highlight the importance of considering the surface properties and particle shapes in evaluating their toxicities. Regarding biological studies for growth inhibition effects, the α-Ag_2WO_4 was evaluated as a microbicidal agent, where the minimum inhibitory concentration (MIC) and the minimum fungicidal concentrations (MFC) were reported with values of 62.5 μg ml^{-1} for *C. albicans* (Foggi et al., 2017a). Another study evaluated the ability of α-Ag_2WO_4 to fight *C. albicans*, with a MIC/MFC value of 7.81 μg ml^{-1} (Foggi et al., 2017b). Comparing these growth data with our results, we found that α-Ag_2WO_4 was substantially more toxic to *R. subcapitata* than to the fungus. In addition, comparing the IC_{50} values of the microparticles with other studies, we found that α-Ag_2WO_4 (cubic and rod) affected *R. subcapitata* growth more than the smaller particle sizes. For example, Ribeiro et al. (2015), when evaluating the toxicity of silver nanoparticles (AgNPs), found IC_{50}-72 h value for *R. subcapitata* of 32.40 μg L^{-1}. Sohn et al. (2015) observed that *R. subcapitata* exposed to silver nanowires (AgNWs) and AgNPs showed IC_{50}-72 h values of 2.57 mg L^{-1} and 0.74 mg L^{-1}, respectively. All these values are higher than the IC_{50}-96 h for α-Ag_2WO_4–C and α-Ag_2WO_4 – R calculated in our study, which points out that the α-Ag_2WO_4, even as a microcrystal, has a higher toxicity to *R. subcapitata* than that found for nanoparticles in the above cited studies. This result can be explained because the α-Ag_2WO_4 semiconductor has a high capacity to produce ROS (OH* and O_2H*), which leads to a high oxidative stress for living organisms (Assis et al., 2019).

The IC_{50}-96 h calculated based on the concentration of free Ag from α-Ag_2WO_4–C and α-Ag_2WO_4 - R were 3.94 μg Ag L^{-1} and 4.76 μg Ag L^{-1}, respectively. These values are consistent with the EC_{50} values described in the literature for *R. subcapitata* exposed to dissolved Ag, for example, the EC_{50} of 3.6 μg L^{-1} reported by Sekine et al. (2015). Thus, the toxicity of both microparticles in our study can be explained by the release of Ag^+ ions. It is important to note that in Brazil the CONAMA determines 10 μg L^{-1} of ionic silver as an adequate threshold to maintain freshwater quality (BRASIL, 2005). Our results show that concentrations of ionic silver from microcrystals lower than those established by Brazilian legislation can impact freshwater microalgae. This reinforces the importance of investigating the toxicity of functional microparticle-based materials to aquatic organisms, especially organisms that make up the base of the trophic chain, because the aquatic ecosystem can be an important fate for the microcrystals and the ions released by them.

3.1.2. ROS measurements

After 24 h of exposure to α-Ag_2WO_4–C, we observed a significant increase in the amount of relative ROS in algal cells exposed to concentrations of 8.81 and 19.32 μg L^{-1} (Dunnett's test, $p < 0.05$). At 96 h, the relative ROS decreased significantly at concentrations of 8.81, 19.32, and 27.78 μg L^{-1} (Dunnett's test, $p < 0.05$) (Fig. 4A). For α-Ag_2WO_4 - R, at 96 h there was a significant reduction in intracellular ROS content at concentrations 10.55 and 10.67 μg L^{-1} (Dunnett's test, $p < 0.05$) and a significant increase at the highest concentration tested (Dunnett's test, $p < 0.05$) when compared to the control. (Fig. 4B).

The formation of intracellular ROS can be induced in the presence of light, that is, mediated by photocatalytic properties of the materials (Nadia von Moss and Slaveykova, 2013; Vale et al., 2016). Therefore, we can state that the ROS production by microalgae was induced by exposure to α-Ag_2WO_4. Foggi et al. (2017a) reported that ROS can influence the cell death of *C. albicans* exposed to α-Ag_2WO_4. Thus, the authors considered the ROS production an important route of toxicity.

We observed that significant relative ROS production was closely linked with growth inhibition at the highest concentration (31.76 μg L^{-1}) of α-Ag_2WO_4-R. ROS can act as signaling molecules and alter gene expression, besides causing modifications in nucleic acids, proteins and lipids, and cell damage (Okamoto et al., 2003), and, therefore, we suggest that ROS generation was responsible for the total growth inhibition after 96 h exposure. High levels of ROS, when the antioxidant limit of the cell is exceeded, can cause disorderly oxidation of biological and cellular molecules, leading to oxidative stress with changes in cell structure (Halliwell and Gutteridge, 1999), cell disruption, and death (Nadia von Moss and Slaveykova, 2013; Taylor et al., 2015; Vale et al., 2016). According to Okamoto et al. (2003), the formation of ROS in autotrophs is a serious risk, because a source of $O^{\cdot}_2$-is the reduction of a single electron of molecular oxygen by the electron transport chain. In addition, mitochondria and chloroplasts are vulnerable to oxidative damage.

However, microalgae have antioxidant mechanisms that are activated when excessive ROS production occurs, as reported by Lekamge et al. (2019). These researchers observed the activation of antioxidant enzymes when *R. subcapitata* was exposed to particles with silver. Moreover, it was reported that *Chlorella vulgaris* could continue photosynthesis at high concentrations of silver nanoparticles, because it was able to activate antioxidant enzymes and detoxify the reactive oxygen species (Qian et al., 2016). This may explain the reduction of relative ROS at some concentrations after 96 h of microcrystal exposure. The Chlorophyceae exposed to α-Ag_2WO_4 may have activated these antioxidant mechanisms and decreased ROS content at concentrations of 8.81, 19.32, and 27.78 μg L^{-1} for α-Ag_2WO_4–C and 10.55 and 10.67 μg L^{-1} for α-Ag_2WO_4-R (Fig. 4A and B). This significant reduction in ROS is corroborated by the growth data, where no complete inhibition at these same concentrations were observed. We emphasize that we did not evaluate and quantify these antioxidant enzymes, but they were possibly activated due to the stress state caused by the microcrystal.

3.1.3. Cell complexity, size and chlorophyll a fluorescence

For *R. subcapitata* exposed to α-Ag_2WO_4– C, we verified morphological changes when compared to the control (Fig. 5A**).** There was a significant reduction (Dunnett's test, $p < 0.05$) in cell complexity (SSC–H) at concentrations of 8.81 and 19.32 μg L^{-1} and a significant increase (Dunnett's test, $p < 0.05$) at concentrations of 27.78, 32.87, and 36.25 μg L^{-1}. For α-Ag_2WO_4- R, there was a significant increase (Dunnett's test, $p < 0.05$) in cell complexity (SSC–H) at the highest concentration (31.76 μg L^{-1}) and a reduction in other concentrations, which were also statistically significant (Dunnett's test, $p < 0.05$). There were no statistically significant differences for cell size (FSC–H) exposed to α-Ag_2WO_4– C and α-Ag_2WO_4- R.

The increase in complexity observed in some concentrations of α-Ag_2WO_4– C (27.78, 32.87, and 36.25 μg L^{-1}) and at the highest concentration of α-Ag_2WO_4 - R is probably a result of the internalization of

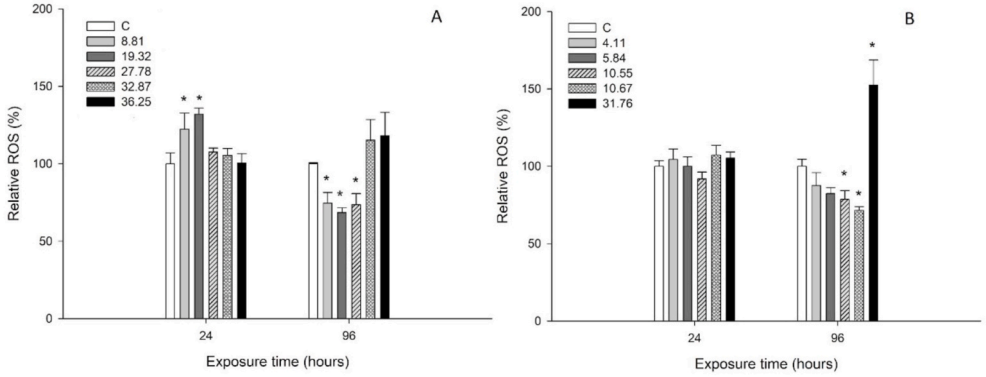

Fig. 4. Reactive oxygen species (ROS) produced by *Raphidocelis subcapitata* exposed to α-Ag_2WO_4–C (A) and α-Ag_2WO_4 - R (B). Concentrations are expressed in μg L^{-1}, where: C = control group and asterisks represent a significant difference (Dunnett's test, $p < 0.05$) of treatments compared to the control group.

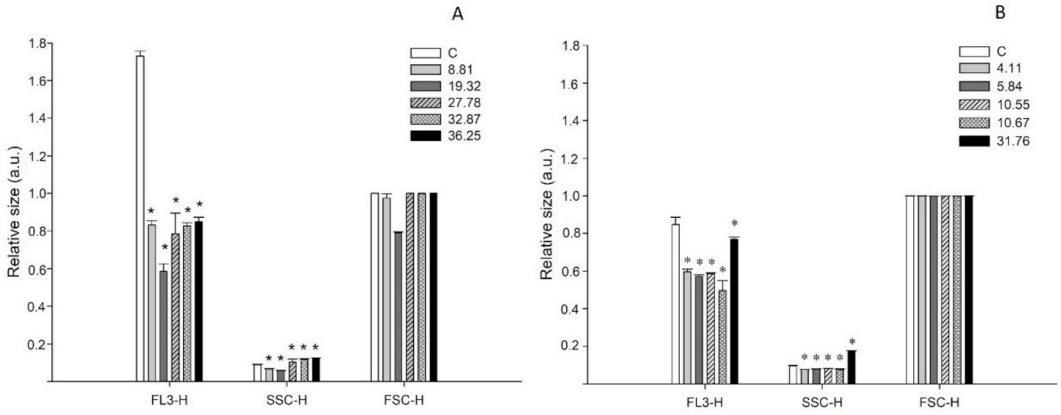

Fig. 5. Chlorophyll *a* fluorescence (FL3-H relative), cell complexity (SSC–H relative) and size (FSC–H relative) (mean ± standard deviation) of *Raphidocelis subcapitata* exposed to the different concentrations of α-Ag_2WO_4–C (A) and α-Ag_2WO_4 – R (B). Concentrations are expressed in μg L^{-1}, where: C = control group and asterisks represent a significant difference (Dunnett's test, $p < 0.05$) of treatments compared to the control group. Values are expressed in arbitrary units (a.u.).

ionic silver, as already observed for other metals (Gebara et al., 2020). Almeida et al. (2019) reported that cell granularity changes may represent detoxification mechanisms through the immobilization of toxic elements inside the cell. Specifically, for the highest concentration of rod microparticle (31.76 μg L^{-1}), the cell complexity results corroborate the relative ROS and growth inhibition data for this treatment, indicating that ion internalization (observed by increased cell complexity) was directly related to the significant increase in ROS and complete inhibition of cell growth. On the other hand, reduced cell complexity was associated with significantly reduced ROS, for α-Ag_2WO_4–C (at concentrations 8.81 and 19.32 μg L^{-1}) and α-Ag_2WO_4 - R. This is a strong indication that the cells exposed to the different microcrystal morphologies activated defense mechanisms, with reduced cell complexity, relative ROS reduction, and no complete inhibition of cell growth.

Regarding Chl *a* fluorescence (FL3-H) for both microparticle morphologies, there was a statistically significant reduction (Dunnett's test, $p < 0.05$) in FL3-H at all concentrations tested (Fig. 5A and B). This reduction possibly indicates that exposure to α-Ag_2WO_4 affected pigment synthesis. Sendra et al. (2017) highlighted that fluorescence measured with FL3 detector can be used as an indicator in assessing the physiological state of algal cells and also pointed out that the reduction in FL3 is related to impairment in pigment synthesis of cells exposed to contaminants. Thus, we assume that the decreased Chl *a* production may have caused consequences to the microalga photosynthetic performance, contributing to population growth inhibition.

4. Conclusion

Our results showed that both morphologies of α-Ag_2WO_4 caused population growth inhibition, changes in cell morphology (cell complexity) and, at the intracellular level, induced ROS production and reduced Chl *a* fluorescence. The α-Ag_2WO_4 – R showed greater toxicity to algal cells than α-Ag_2WO_4–C, caused by differences in the surface energy of each crystal, which are closely related to the number of active sites. In addition, silver ions are important sources and seem to be responsible for the toxicity, deserving attention, because the limit set by legislation for ionic silver in aquatic ecosystems is higher than the concentration of silver that caused toxicity for freshwater alga. We emphasize that particle shape is an intrinsic and essential aspect in assessing the toxicity of microparticle-based functional materials, because its reactivity is also conditioned by morphology and surface area. Considering that the aquatic ecosystem is an important fate of contaminants, we highlight the importance of this investigation in providing subsidies for a better understanding of the toxicity of α-Ag_2WO_4 and the potential risks that compounds in different morphologies may pose to microalgae, supporting regulatory actions to establish safe thresholds for these compounds and silver ions.

Author contributions

This manuscript describes original work and is not under consideration by any other journal. All authors assume that they have read the final version of the manuscript and agreed with it. The contribution of each author of this work is described below: CBA: co-developed the

experimental design, carried out experimental tests and collected the data; performed statistical analysis; analyzed and interpreted the data and wrote the paper. RCG: co-developed the experimental design, carried out experimental tests and collected the data; performed statistical analysis; analyzed and interpreted the data and reviewed the paper. LLR: carried out experimental tests, collected the data and reviewed the paper. GSR: carried out experimental tests and collected the data; performed statistical analysis; analyzed and interpreted the data and reviewed the paper. LGOA: analyzed and interpreted the data and reviewed the paper. LMA: performed the characterization of α-Ag_2WO_4 and reviewed the paper. LSV: performed the characterization of α-Ag_2WO_4 and reviewed the paper. MA: co-developed the experimental design; analyzed and interpreted the data and reviewed the paper. ASM: co-developed the experimental design; performed statistical analysis, analyzed and interpreted the data and reviewed the paper. EL: co-developed the experimental design; analyzed and interpreted the data and reviewed the paper. This author is also one of the sponsors, responsible for obtaining financial grant that supported this study (FAPESP CEPID-finance code 2013/07296–2). MGGM: co-developed the experimental design; analyzed and interpreted the data and reviewed the paper. This author is also one of the sponsors, responsible for obtaining financial grant that supported this study (FAPESP, 2018/07988–5).

Declaration of competing interest

The authors declare that they have no known competing financial interests or personal relationships that could have appeared to influence the work reported in this paper.

Acknowledgements

This work was funded in part São Paulo Research Foundation (FAPESP) (FAPESP CEPID-finance code 2013/07296-2; finance code 2018/07988-5), Financier of Studies and Projects (FINEP), National Council for Scientific and Technological Development (CNPq) (finance code 166281/2017-4 and 141255/2018-8), and Coordination for the Improvement of Higher Education Personnel (CAPES) (finance code 001 and 88887.364036/2019–00). We would also like to thank Dr. Ana Teresa Lombardi and Dr. Hugo Miguel Preto de Morais Sarmento for the permission to use their laboratories, as well as the equipment.

Appendix A. Supplementary data

Supplementary data to this article can be found online at https://doi.org/10.1016/j.chemosphere.2021.132536.

References

Almeida, C., Gomes, T., Habuda-Stanic, M., Lomba, J.A.B., Romić, Željka, Turkalj, J.V., Lillicrap, A., 2019. Characterization of multiple biomarker responses using flow cytometry to improve environmental hazard assessment with the green microalgae *Raphidocelis subcapitata*. Science of the Total Environment journal 687, 827–838. https://doi.org/10.1016/j.scitotenv.2019.06.124.

Alvarez-Roca, R., Gouveia, A.F., De Foggi, C.C., Lemos, P.S., Gracia, L., Silva, L.F., Vergani, C.E., San-Miguel, M., Longo, E., Andrés, J., 2021. Selective synthesis of α-, β-, and γ-Ag2WO4 polymorphs: promising platforms for photocatalytic and antibacterial materials. Inorg. Chem. 60, 1062–1079. https://doi.org/10.1021/acs.inorgchem.0c03186.

Arumugam, R., Osman, S., Pan, J., Khan, A., Yang, V., 2020. One-pot preparation of AgBr/α-Ag_2WO_4 composite with superior photocatalytic activity under visible-light irradiation. Colloids Surf., A 586, 124079. https://doi.org/10.1016/j.colsurfa.2019.124079.

Assis, M., Cordoncillo, E., Torres-Mendieta, R., Beltrán-Mir, H., Mínguez-Vega, G., Oliveira, R., Leite, E.R., Foggi, C.C., Vergani, C.E., Longo, E., Andrés, J., 2018. Towards the scale-up of the formation of nanoparticles on α-Ag2WO4with bactericidal properties by femtosecond laser irradiation. Sci. Rep. 8, 1–11. https://doi.org/10.1038/s41598-018-19270-9.

Assis, M., Robeldo, T., Foggi, C.C., Kubo, A.M., Condoncillo, E., 2019. Composite Formed by Electron Beam and Femtosecond Irradiation as Potent Antifungal and Antitumor Agents 1–15. https://doi.org/10.1038/s41598-019-46159-y.

Assis, M., Pontes Ribeiro, R.A., Carvalho, M.H., Teixeira, M.M., Gobato, Y.G., Prando, G. A., Mendonça, C.R., De Boni, L., Aparecido De Oliveira, A.J., Bettini, J., Andrés, J., Longo, E., 2020. Unconventional magnetization generated from electron beam and femtosecond irradiation on α-Ag_2WO_4: a quantum chemical investigation. ACS Omega 5, 10052–10067. https://doi.org/10.1021/acsomega.0c00542.

Assis, M., Ponce, M.A., Gouveia, A.F., Souza, D., de Campos da Costa, J.P., Teodoro, V., Gobato, Y.G., Andres, J., Macchi, C., Somoza, A., Longo, E., 2021. Revealing the nature of defects in α-Ag2WO4 by positron annihilation lifetime spectroscopy: a joint experimental and theoretical study. Cryst. Growth Des. 21, 1093–1102. https://doi.org/10.1021/acs.cgd.0c01417.

Ayappan, C., Jayaraman, V., Palanivel, B., Pandikumar, A., 2020. Separation and Puri fi cation Technology Facile preparation of novel Sb_2S_3 nanoparticles/rod-like α -Ag_2WO_4 heterojunction photocatalysts : continuous modulation of band structure towards the e ffi cient removal of organic contaminants. Separ. Purif. Technol. 236, 116302. https://doi.org/10.1016/j.seppur.2019.116302.

Bao, V.W.W., Leung, K.M.Y., Qiu, J.W., Lam, M.H.W., 2011. Acute toxicities of five commonly used antifouling booster biocides to selected subtropical and cosmopolitan marine species. Mar. Pollut. Bull. 62, 1147–1151. https://doi.org/10.1016/j.marpolbul.2011.02.041.

Beer, C., Foldbjerg, R., Hayashi, Y., Sutherland, D.S., Autrup, H., 2012. Toxicity of silver nanoparticles-Nanoparticle or silver ion? Toxicol. Lett. 208, 286–292. https://doi.org/10.1016/j.toxlet.2011.11.002.

BRASIL, 2005. Ministério Do Meio Ambiente. Conselho Nacional Do Meio Ambiente CONAMA. Resoluç Ão N0 357 de 17 de marçoo de 2005. Diário Oficial da União, Brasília.

Cavalcante, L.S., Almeida, M.A.P., Avansi, W., Tranquilin, R.L., Longo, E., Batista, N.C., Paulista, U.E., Box, P.O., 2012. Cluster Coordination and Photoluminescence Properties of. https://doi.org/10.1021/ic300948n.

Chu, S.P., 1942. The influence of the mineral composition of the medium on the growth of planktonic algae: Part I. Methods and culture media. J. Ecol. 30, 284. https://doi.org/10.2307/2256574.

Cruz, L., Teixeira, M.M., Teodoro, V., Jacomaci, N., Laier, L.O., Assis, M., Macedo, N.G., Tello, A.C.M., Da Silva, L.F., Marques, G.E., Zaghete, M.A., Teodoro, M.D., Longo, E., 2020. Multi-dimensional architecture of Ag/α-Ag2WO4crystals: insights into microstructural, morphological, and photoluminescence properties. CrystEngComm 22, 7903–7917. https://doi.org/10.1039/d0ce00876a.

Dai, X., Luo, Y., Zhang, W., Fu, S., 2010. Facile Hydrothermal Synthesis and Photocatalytic Activity of Bismuth Tungstate Hierarchical Hollow Spheres with an Ultrahigh Surface Area, pp. 3426–3432. https://doi.org/10.1039/b923443h.

Dobias, J., Bernier-Latmani, R., 2013. Silver release from silver nanoparticles in natural waters. Environ. Sci. Technol. 47 (9), 4140–4146. https://doi.org/10.1021/es304023p.

Fabrega, J., Fawcett, S.R., Renshaw, J.C., Lead, J.R., 2009. Silver nanoparticle impact on bacterial growth: effect of pH, concentration, and organic matter. Environ. Sci. Technol. 43, 7285–7290. https://doi.org/10.1021/es803259g.

Foggi, C.C., Fabbro, M.T., Santos, L.P.S., de Santana, Y.V.B., Vergani, C.E., Machado, A. L., Cordoncillo, E., Andrés, J., Longo, E., 2017a. Synthesis and evaluation of A-Ag_2WO_4 as novel antifungal agent. Chem. Phys. Lett. 674, 125–129. https://doi.org/10.1016/j.cplett.2017.02.067.

Foggi, C.C., de Oliveira, R.C., Fabbro, M.T., Vergani, C.E., Andres, J., Longo, E., Machado, A.L., 2017b. Tuning the morphological, optical, and antimicrobial properties of α-Ag_2WO_4 microcrystals using different solvents. Cryst. Growth Des. 17, 6239–6246. https://doi.org/10.1021/acs.cgd.7b00786.

Gebara, R.C., Alho, L.O.G., Rocha, G.S., Mansano, A.S., Melão, M.G.G., 2020. Zinc and aluminum mixtures have synergic effects to the algae *Raphidocelis subcapitata* at environmental concentrations. Chemosphere 242, 125231. https://doi.org/10.1016/j.chemosphere.2019.125231.

Griffitt, R.J., Brown-Peterson, N.J., Savin, D.A., Manning, C.S., Boube, I., Ryan, R.A., Brouwer, M., 2012. Effects of chronic nanoparticulate silver exposure to adult and juvenile sheepshead minnows (*Cyprinodon variegatus*). Environ. Toxicol. Chem. 31, 160–167. https://doi.org/10.1002/etc.709.

Halliwell, B., Gutteridge, J.M.C., 1999. Free Radicals in Biology and Medicine., 3rd. Oxford University Press, New York, p. 936pp.

He, D., Dorantes-Aranda, J.J., Waite, T.D., 2012. Silver nanoparticle-algae interactions: oxidative dissolution, reactive oxygen species generation and synergistic toxic effects. Environ. Sci. Technol. 46, 8731–8738. https://doi.org/10.1021/es300588a.

Hong, Y., Hu, H., Xie, X., Sakoda, A., Sagehashi, M., Li, F., 2009. Gramine-induced growth inhibition , oxidative damage and antioxidant responses in freshwater cyanobacterium *Microcystis aeruginosa*. Aquatic Toxicology 91, 262–269. https://doi.org/10.1016/j.aquatox.2008.11.014.

Kleiven, M., Rossbach, L.M., Gallego-Urrea, J.A., Brede, D.A., Oughton, D.H., Coutris, C., 2018. Characterizing the behavior, uptake, and toxicity of NM300K silver nanoparticles in *Caenorhabditis elegans*. Environ. Toxicol. Chem. 37, 1799–1810. https://doi.org/10.1002/etc.4144.

Huang, J., Cheng, J., Yi, J., 2016. Impact of silver nanoparticles on marine diatom *Skeletonema costatum*. J. Appl. Toxicol. https://doi.org/10.1002/jat.3325.

Kleiven, M., Macken, A., Oughton, D.H., 2019. Chemosphere Growth inhibition in *Raphidocelis subcapita* e Evidence of nanospecific toxicity of silver nanoparticles. Chemosphere 221, 785–792. https://doi.org/10.1016/j.chemosphere.2019.01.055.

Kwak, J.II, Cui, R., Sun-Hwa, N., Kim, S.W., Chae, Y., An, Y.J., 2015. Multispecies toxicity test for silver nanoparticles to derive hazardous concentration based on species sensitivity distribution for the protection of aquatic ecosystems. Nanotoxicology 5390. https://doi.org/10.3109/17435390.2015.1090028.

Laier, L.O., Assis, M., Foggi, C.C., Gouveia, A.F., Vergani, C.E., Santana, L.C.L., Cavalcante, L.S., Andrés, J., Longo, E., 2020. Surface - dependent properties of α -

Ag_2WO_4 : a joint experimental and theoretical investigation. Theor. Chem. Acc. 1–11 https://doi.org/10.1007/s00214-020-02613-z.
Lalau, C.M., Simioni, C., Vicentini, D.S., Ouriques, L.C., Mohedano, R.A., Puerari, R.C., Matias, W.G., 2020. Science of the total environment toxicological effects of AgNPs on duckweed (*Landoltia punctata*). Sci. Total Environ. 710, 136318. https://doi.org/10.1016/j.scitotenv.2019.136318.
Lekamge, S., Miranda, A.F., Abraham, A., Ball, A.S., Shukla, R., Nugegoda, D., 2020. The toxicity of coated silver nanoparticles to the alga *Raphidocelis subcapitata*. SN Appl. Sci. https://doi.org/10.1007/s42452-020-2430-z.
Lin, C.A.O., Jiexin, C.A.O., Cong, W., Ping, C.H.E., An, P.A.N.D.E., Volinsky, A.A., 2012. Anti-tumor activity of self-charged (Eu, Ca): WO3 and Eu : CaWO4 Nanoparticles. Bull. Mater. Sci. 35, 767–772.
Lodeiro, P., Browning, T.J., Achterberg, E.P., Guillou, A., El-Shahawi, M.S., 2017. Mechanisms of silver nanoparticle toxicity to the coastal marine diatom *Chaetoceros curvisetus*. Sci. Rep. 7, 1–10. https://doi.org/10.1038/s41598-017-11402-x.
Lopes, S., Ribeiro, F., Wojnarowicz, J., Lojkowski, W., Jurkschat, K., Crossley, A., Soares, A.M.V.M., Loureiro, S., 2014. Zinc oxide nanoparticles toxicity to *Daphnia magna*: size-dependent effects and dissolution. Environ. Toxicol. Chem. 33, 190–198. https://doi.org/10.1002/etc.2413.
Macedo, N.G., Gouveia, A.F., Roca, R.A., Assis, M., Gracia, L., Andre, J., Leite, E.R., Longo, E., Box, P.O., 2018. Surfactant-Mediated Morphology and Photocatalytic Activity of α-Ag_2WO_4 Material. https://doi.org/10.1021/acs.jpcc.8b01898.
Macedo, N.G., MacHado, T.R., Roca, R.A., Assis, M., Foggi, C.C., Puerto-Belda, V., Mínguez-Vega, G., Rodrigues, A., San-Miguel, M.A., Cordoncillo, E., Beltrán-Mir, H., Andrés, J., Longo, E., 2019. Tailoring the bactericidal activity of Ag nanoparticles/α-Ag_2WO_4 composite induced by electron beam and femtosecond laser irradiation: integration of experiment and computational modeling. ACS Appl. Bio Mater. 2, 824–837. https://doi.org/10.1021/acsabm.8b00673.
Mansano, A.S., Vieira, E.M., Sarmento, H., Rocha, O., Seleghim, M.H.R., 2017. Effects of diuron and carbofuran and their mixtures on the microalgae *Raphidocelis subcapitata*. Ecotoxicol. Environ. Saf. 142, 312–321. https://doi.org/10.1016/j.ecoenv.2017.04.024.
Moos, N. Von, Slaveykova, V.I., 2013. Oxidative stress induced by inorganic nanoparticles in bacteria and aquatic microalgae – state of the art and knowledge gaps. Nanotoxicology 1–26. https://doi.org/10.3109/17435390.2013.809810.
Munawar, M., Munawar, I.F., Mayfield, C.I., McCarthy, L.H., 1990. Probing ecosystem health: a multi-disciplinary and multi-trophic assay strategy. Environ. bioassay Tech. their Appl. Proc. Conf. Lancaster 93–116. https://doi.org/10.1007/978-94-009-1896-2_8, 1988.
Muthamizh, S., Suresh, R., Giribabu, K., Manigandan, R., Praveen Kumar, S., Munusamy, S., Narayanan, V., 2015. $MnWO_4$nanocapsules: synthesis, characterization and its electrochemical sensing property. J. Alloys Compd. 619, 601–609. https://doi.org/10.1016/j.jallcom.2014.09.049.
Navarro, E., Baun, A., Behra, R., Hartmann, N.B., Filser, J., Miao, A.J., Quigg, A., Santschi, P.H., Sigg, L., 2008. Environmental behavior and ecotoxicity of engineered nanoparticles to algae, plants, and fungi. Ecotoxicology 372–386. https://doi.org/10.1007/s10646-008-0214-0.
Nobre, F.X., Bastos, I.S., dos Santos Fontenelle, R.O., Júnior, E.A.A., Takeno, M.L., Manzato, L., de Matos, J.M.E., Orlandi, P.P., de Fátima Souza Mendes, J., Brito, W. R., da Costa Couceiro, P.R., 2019. Antimicrobial properties of α-Ag_2WO_4 rod-like microcrystals synthesized by sonochemistry and sonochemistry followed by hydrothermal conventional method. Ultrason. Sonochem. 58, 104620. https://doi.org/10.1016/j.ultsonch.2019.104620.
Odzak, N., Kistler, D., Sigg, L., 2017. In fl uence of daylight on the fate of silver and zinc oxide nanoparticles in natural aquatic environments. Environ. Pollut. 226, 1–11. https://doi.org/10.1016/j.envpol.2017.04.006.
Oecd, O., 2011. Guidelines for the testing of chemicals No. 201 freshwater alga and cyanobacteria. Growth Inhibition Test 201.
Okamoto, O.K., Qu, I. De, Morse, D., 2003. Review heavy metal – induced oxidative stress in Algae. J. Phycol. 1018, 1008–1018.
Penha, M.D., Gouveia, A.F., Teixeira, M.M., De Oliveira, R.C., Assis, M., Sambrano, J.R., Yokaichya, F., Santos, C.C., Goncalves, R.F., Li, M.S., 2020. Structure, optical properties, and photocatalytic activity of α-Ag2W0. 75Mo0. 25O4. Mater. Res. Bull. 132, 111011.
Qian, H., Zhu, K., Lu, H., Lavoie, M., Chen, S., Zhou, Z., Deng, Z., Chen, J., Fu, Z., 2016. Contrasting silver nanoparticle toxicity and detoxification strategies in *Microcystis aeruginosa* and *Chlorella vulgaris*: New insights from proteomic and physiological analyses. Sci. Total Environ. 572, 1213–1221. https://doi.org/10.1016/j.scitotenv.2016.08.039.
Reis, L.L., Alho, L.O.G., Abreu, C.B., Melão, M.G.G., 2021. Using Multiple Endpoints to Assess the Toxicity of Cadmium and Cobalt for Chlorophycean *Raphidocelis subcapitata*. Ecotoxicol. Environ. Saf 208, 111628. https://doi.org/10.1016/j.ecoenv.2020.111628.
Ribeiro, F., Gallego-Urrea, J.A., Goodhead, R.M., Van Gestel, C.A.M., Moger, J., Soares, A.M.V.M., Loureiro, S., 2015. Uptake and elimination kinetics of silver nanoparticles and silver nitrate by *Raphidocelis subcapitata*: The influence of silver behaviour in solution. Nanotoxicology 9. https://doi.org/10.3109/17435390.2014.963724.
Rogers, K.R., Navratilova, J., Stefaniak, A., Bowers, L., Knepp, A.K., Al-Abed, S.R., Potter, P., Gitipour, A., Radwan, I., Nelson, C., Bradham, K.D., 2018. Characterization of engineered nanoparticles in commercially available spray disinfectant products advertised to contain colloidal silver. Sci. Total Environ. 619–620, 1375–1384. https://doi.org/10.1016/j.scitotenv.2017.11.195.
Sarmento, H., Unrein, F., Isumbisho, M., Stenuite, S., Gasol, J.M., Descy, J.P., 2008. Abundance and distribution of picoplankton in tropical, oligotrophic Lake Kivu, eastern Africa. Freshw. Biol. 756–771. https://doi.org/10.1111/j.1365-2427.2007.01939.x.
Sekine, R., Khurana, K., Vasilev, K., Lombi, E., Donner, E., 2015. Quantifying the adsorption of ionic silver and functionalized nanoparticles during ecotoxicity testing: Test container effects and recommendations. Nanotoxicology 5390, 1–8. https://doi.org/10.3109/17435390.2014.994570.
Sendra, M., Yeste, M.P., Gatica, J.M., Blasco, J., 2017. Direct and indirect effects of silver nanoparticles on freshwater and marine microalgae (*Chlamydomonas reinhardtii* and *Phaeodactylum tricornutum*). Chemosphere. https://doi.org/10.1016/j.chemosphere.2017.03.123.
Silva, L.F., Catto, A.C., Avansi, W., Cavalcante, L.S., Andrés, J., Aguir, K., Mastelaro, V.R., Longo, E., 2014. A novel ozone gas sensor based on one-dimensional (1D) α-Ag $_2WO_4$ nanostructures. Nanoscale 6, 4058–4062. https://doi.org/10.1039/c3nr05837a.
Silva, L.F., Catto, A.C., Avansi, W., Cavalcante, L.S., Mastelaro, V.R., Andrés, J., Aguir, K., Longo, E., 2016. Acetone gas sensor based on α-Ag_2WO_4 nanorods obtained via a microwave-assisted hydrothermal route. J. Alloys Compd. 683, 186–190. https://doi.org/10.1016/j.jallcom.2016.05.078.
Sohn, E.K., Johari, S.A., Kim, T.G., Kim, E., Lee, J.H., Chung, Y.S., yu, IIJ., 2015. Aquatic Toxicity Comparison of Silver Nanoparticles and Silver Nanowires. Biomed Res Int. https://doi.org/10.1155/2015/893049.
Sørensen, S.N., Lützhøft, H.H., Rasmussen, R., Baun, A., 2016. Acute and chronic effects from pulse exposure of *D. magna* to silver and copper oxide nanoparticles. Aquat. Toxicol. https://doi.org/10.1016/j.aquatox.2016.10.004.
Stensberg, M.C., Wei, Q., Mclamore, E.S., Marshall, D., 2011. Toxicological studies on silver nanoparticles: challenges and oopportunities in assessment, monitoring and imaging. Nanomedicine 6, 879–898. https://doi.org/10.2217/nnm.11.78.
Statsoft Inc, 2004. STATISTICA, Version 07. www.statsoft.com.
Systat, 2008. Systat Software, Incorporation SigmaPlot for Windows version 11.0.
Taylor, P., Street, M., Wt, L., 2015. Toxicity , bioaccumulation and biomagnification of silver nanoparticles in green algae (*Chlorella* sp.), water flea (Moina macrocopa), blood worm (Chironomus spp.) and silver barb (Barbonymus goniono 37–41. sp. https://doi.org/10.3184/095422914X14144332205573.
Vale, Gonçalo, Mehennaouic, K., Cambierc, S., Libralatod, G., Jominie, S., Domingosa, R. F., 2015. Manufactured nanoparticles in the aquatic environment – biochemical responses on freshwater organisms : a critical overview. Aquat. Toxicol. 170, 162–174. https://doi.org/10.1016/j.aquatox.2015.11.019.
Varga, A.M., Horvati, J., 2018. Physiological and biochemical effect of silver on the aquatic plant Lemna gibba L.: evaluation of commercially available product containing colloidal silver. Aquat. Toxicol. https://doi.org/10.1016/j.aquatox.2018.11.018.
Wang, S., Lv, J., Ma, J., Zhang, S., 2016. Cellular internalization and intracellular biotransformation of silver nanoparticles in *Chlamydomonas reinhardtii*. Nanotoxicology 10, 1129–1135. https://doi.org/10.1080/17435390.2016.1179809.
Zhao, C., Wang, W., 2012. Importance of surface coatings and soluble silver in silver nanoparticles toxicity to *Daphnia magna*. Nanotoxicology 6, 361–370. https://doi.org/10.3109/17435390.2011.579632.